J. Meas. Sci. Instrum., 2022, 13(2): 242-252
DOI: 10.3969/j.issn.1674-8042.2022.02.014
http://xuebao.nuc.edu.cn
jmsi@nuc.edu.cn

Comparison of electromagnetic exposure to child and adult from electric vehicle wireless power transmission

KANG Haixia

(*Key Laboratory of Opto-Technology and Intelligent Control of Ministry of Education, Lanzhou Jiaotong University, Lanzhou 730070, China*)

Abstract: It is important to verify the safety of electric vehicle (EV) wireless power transmission for child passengers by studying the electromagnetic exposure difference between the child passengers and the adult passengers. The dielectric parameters of the child passengers' body were calculated under the operating frequency of 85 kHz. Using the finite element simulation software COMSOL Multiphysics, a model was established for the child passengers and adult passengers when the EVs charged by the wireless charging coil. This paper analyzed the distribution of magnetic induction intensity and induced electric field intensity generated on the body and head when the child passengers and adult passengers sat in four different positions. Additionally, the difference between the brain electromagnetic exposure values of children and adults was analyzed and compared with the limits set. The results showed that the electromagnetic exposure was the largest when the passenger sat in the co-driver position. The electromagnetic exposure level of child was slightly higher than that of adult at the same position, and the magnetic induction intensity and induced electric field intensity of both were much smaller than the public electromagnetic exposure recommendation values.

Key words: electric vehicle; electromagnetic exposure; child model; wireless charging coil; finite element methods

0 Introduction

With the intensification of the global greenhouse effect and the increasingly prominent energy problems, the emergence of electric vehicles (EVs) has brought new hope and development points for the mitigation of environmental degradation. It is a tendency that the EVs will replace traditional fuel vehicles due to its environmental protection and zero emissions[1-2]. However, the subsequent electromagnetic exposure problem has attracted public attention. The wireless charging technology effectively solves various problems of contact charging, such as risk of sparks, electric shock dust and contact losses in harsh environments, and has been researched and applied widely. With the further research of EV wireless charging technology[3-4], its electromagnetic safety problems have recently became one of the research hotspots.

Many studies have been conducted on electromagnetic exposure safety problems of EV wireless power transmission. The Massachusetts Institute of Technology (MIT) proposed a magnetically coupled resonant wireless power transmission (WPT) technology suitable for mid-range power transmission in 2007, and they said that the strength of the magnetic field between the two resonant coils was the same as the strength of the geomagnetic field, and it had a negligible effect on human body[5]. Laakso I studied a computational method to calculate the specific absorption rate (SAR) due to a wireless power transmission system in the 10 MHz frequency band[6]. When the transmitted power was 7 kW and the frequency of power transmission was 85 kHz, Laakso I simulated the electromagnetic exposure level of human exposure to the electromagnetic field of electric vehicle wireless charging in 2013 — 2014. The strengths of the external magnetic field around the vehicle and the electric field induced in the human body were compared with the exposure limits set in the international human exposure guidelines. It was found that the external magnetic field strength around the vehicle exceeded the magnetic field limit allowed

Received date: 2020-12-28
Foundation items: Department of Edication of Gansu Province (No. 2018D-08)
Corresponding author: KANG Haixia (1643957138 @qq.com)

by international standards, but the electric field induced by the human body was far below the exposure limit[7-9]. SangWook Park studied the electromagnetic exposure level of electric vehicles equipped with a 6.6 kW resonant wireless energy transmission system, and evaluated the specific absorption rate of human models close to the wireless energy transmission system for three exposure situations in 2016, designed a WPT system for charging EVs and evaluated dosimetry for the system in various exposure scenarios. The designed system made a human body in front of the WPT system without shielding, with shielding, with alignment and misalignment between transmitter and receiver, and with a metal plate on the system for vehicle mimic floor pan[10-12]. Yavolovskaya studied the human body exposed to the low-frequency (1 Hz—10 MHz) electromagnetic field generated by the car WPT system by using the TARO human model, analyzed the human exposure level in different realistic scenarios, calculated the vivo induced electric field and compared it with the basic limits of the International Commission on Non-Ionizing Radiation Protection (ICNIRP). It was found that the calculation results were lower than the basic limits of ICNIRP[13-14]. Xu Guizhi studied the electromagnetic exposure of the main organs of the human body during wireless charging of electric vehicles and found that different tissues in human body had different absorption of electromagnetic waves[15]. Gao Yabio investigated the safety issues associated with thermal effects, electromagnetic (EM) interference voltages induced by the magnetic field near, inside and at the center of an EV wireless charging system and magnetic induction intensity[16]. HE Yaqing studied the influence of electromagnetic fields transmitted by wireless charging of EVs on brain waves and neuropsy chological changes[17]. In the preceding research, the main object was concentrated on the electromagnetic exposure of adults in the wireless charging process of EVs. So there is still a lack of research on the electromagnetic exposure of children during the wireless charging.

In summary, the research object of this study was the electromagnetic exposure of children when the EVs were charged by the wireless charging coil. Firstly, the dielectric parameters of the child passenger's body were calculated by using dielectric parameters of pigs as the sources of the 4th Cole-Cole model to simulate the parameters of human, and then they were put into the model materials. Secondly, the finite element software COMSOL was used to establish a simulation model for the child passengers and adult passengers when the EV was charged by the wireless charging coil. The difference in the electromagnetic field distribution of the body and head between the child passenger and the adult passenger during the wireless charging process were studied. Lastly, comparing the simulation results with the corresponding limits in the ICNIRP guidelines, the electromagnetic exposure safety of child passengers during wireless charging of EVs was evaluated. The research could assess the safety of electromagnetic exposure precisely for 11—12 years old passengers, and made some protective recommendations for child passengers.

1 Methods

1.1 Method of wireless energy transfer

As shown in Fig. 1, when the electric vehicle is wirelessly charged, the transmitting circuit generates an alternating magnetic circuit. The alternating magnetic field is induced in the receiving coil, and then the AC power is converted into DC power by the receiving rectifier and output to the battery load[18-19]. During large power transmission, there is a strong magnetic field around the wireless charging coil. The non-thermal effect of electromagnetic exposure on the body has been internationally recognized, and has become a potential safety issue that cannot be ignored. It is necessary to evaluate the electromagnetic safety level of drivers and passengers when wireless charging.

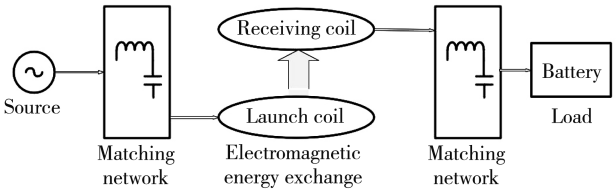

Fig. 1 Wireless charging schematic

In the finite element software, the circuit module is used to simulate the compensation circuit, the magnetic field module is used to simulate the coil entity, and then the field-circuit co-simulation is conducted to simulate the actual wireless charging system as much as possible.

The simplified circuit model is shown in the Fig. 2. Among them, the power supply current is I_s; the primary coil resistance and inductance are R_1 and L_1;

the secondary coil resistance and inductance are R_2 and L_2; C_1 and C_2 are the primary and secondary coil compensation capacitors; R_3 is the load impedance, and M is the coil mutual inductance.

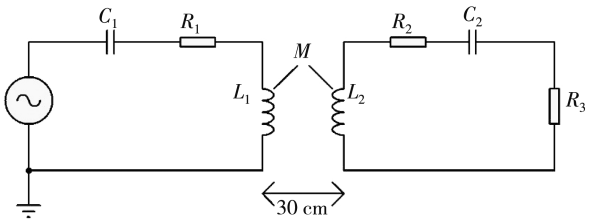

Fig. 2 Simplified circuit model

1.2 Electromagnetic safety related standard

There are a series of standards for electromagnetic exposure safety, mainly containing basic and derived limits. Most developed countries use the guidelines specified by the ICNIRP[20-21] as the basis to limit the safety scope. The ICNIRP guidelines were formally released in 1998, revised in 2010, which stipulated the safety limits for electromagnetic exposure in various organizations within the body of general public and professional personnel. This paper used the frequency of 85 kHz for the wireless charging of electric vehicles to conduct experiments, and then compared results with the ICNIRP reference guidelines. The relevant limits are shown in Table 1.

Table 1 Reference levels for general public exposure to time-varying electric and magnetic fields

Frequency range/kHz	Electric field strength/(V·m^{-1})	Magnetic induction strength/μT
3—150	87	6.25

1.3 Dielectric properties of biological tissues

In bio-electromagnetism, the safety assessment of human exposure to electromagnetic fields requires more accurate human tissue dielectric parameters, i.e. dielectric constant and conductivity. However, due to the limitation of the measurement method, it is difficult to directly measure the parameters of household appliances through experiments, especially the parameters of the central nervous system. Therefore, the currently widely used dielectric parameters in the world are measured in vitro from adults or animals. In 1996, Gabriel measured the relative permittivity and electrical conductivity of 17 kinds of biological tissues through in vitro animal measurement experiments, proposed the 4th Cole-Cole model, and described the dielectric properties of 10 Hz—20 GHz[22-23]. In this paper, the 4th Cole-Cole model were used to calculate the complex dielectric constant.

$$\hat{\varepsilon}_r(\omega) = \varepsilon_\infty + \frac{\sigma_0}{j\omega\varepsilon_0} + \sum_{n=1}^{4} \frac{\Delta\varepsilon_n}{1+(j\omega\tau_n)(1-\alpha_n)}, \quad (1)$$

where ε_∞ is the dielectric constant at infinite frequency; σ_0 is the static ion conductivity; ω is the angular frequency; $\Delta\varepsilon_n$ is the relaxation increment in the dispersion region; τ is the relaxation time; ε_0 is the dielectric constant in free space, and α is the parameter of the dispersion interval distribution. The complex dielectric properties of biological tissues can be expressed as

$$\varepsilon_r = \varepsilon_r' - j\varepsilon_r'', \quad (2)$$

where ε_r' is the real part; ε_r'' is the image part. At the same time, for the complex dielectric constant, the real part is the relative dielectric constant, and the image part is the conductivity. The conductivity is obtained by

$$\sigma = \omega\varepsilon_0\varepsilon_r''. \quad (3)$$

Considering the physical differences between children and adults, as well as the different dielectric parameters of body tissues at different frequency, the absorption characteristics of electromagnetic waves are different, so it is necessary to distinguish the different ages when conducting human electromagnetic exposure and safety assessments. A large number of experimental studies have shown that the dielectric parameters of animals were similar to those of humans. Therefore, the dielectric properties of animal tissues of different ages were compared with those of human tissues at different ages[24-25] for the differences in human electromagnetic exposure. The data used in this paper is the measurement data of pig biological tissues carried out by Peyman et al. in 2001 and 2007. The dielectric parameters of 50 kg pigs were fitted to replace the body dielectric parameters of 11—12 years-old as shown in Table 2.

Table 2 Dielectric parameters of child tissues at 85 kHz

Tissue	Relative dielectric constant	Conductivity /(S·m^{-1})
Scalp	468.99	0.121 1
Skull	261.62	0.200 1
Brain tissue	411.42	0.085 2
Body	340.19	0.110 3

The dielectric parameters of adults are shown in Table 3. The dielectric parameters of brain tissue adopted the average value of brain gray matter and

white matter, and the dielectric parameters of body tissue are reflected by the average value of skin, blood, muscle and bone.

Table 3 Dielectric parameters of adult tissues at 85 kHz

Tissue	Relative dielectric constant	Conductivity /(S·m^{-1})
Scalp	472.57	0.060 1
Skull	117.13	0.120 1
Brain tissue	308.64	0.185 2
Body	284.49	0.031 1

2 Modeling

2.1 Electric vehicle wireless charging system model

The coil model is shown in Fig. 3. The car body model established in this paper is shown in Fig. 4, which is made by alloy steel. The length, width and height are 4.25 m, 1.6 m and 1.5 m. The frequency is 85 kHz. The coil parameters are shown as Table 4.

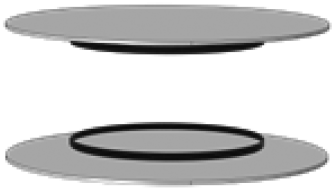

Fig. 3 Coil model

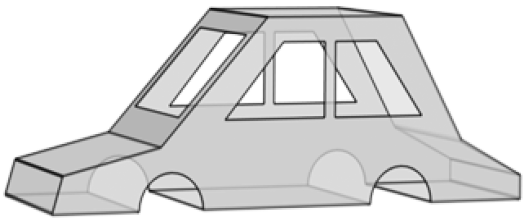

Fig. 4 Electric car model

Table 4 Parameters of coil

Parameter	Value
Ferrite plate radius/cm	50
Coil radius/cm	30
Distance between two coils/cm	30
Primary coil inductance/μH	62
Secondary coil inductance/μH	57
Primary compensation capacitor/nF	56.5
Secondary compensation capacitor/nF	61.5
Input current/A	30
Turns	5

2.2 Human body model

The adult passenger model is shown in Fig. 5(a). According to GB10000-88 Chinese adult human body size, a human model was established with a height of 1.754 m, whose sitting height is 0.947 m. The international standard 3-layer human head model was used[26], with a scalp radius of 0.092 m, a skull radius of 0.085 m, and a brain radius of 0.080 m. The child model is shown in Fig. 5(b). According to GB/T26158—2010 Chinese child body size an 11—12 years-old child model was built, with a height of 1.582 m, whose sitting height was 0.834 m. The radius of the scalp was 0.067 m, the radius of the skull was 0.062 m, and the radius of the brain was 0.058 m.

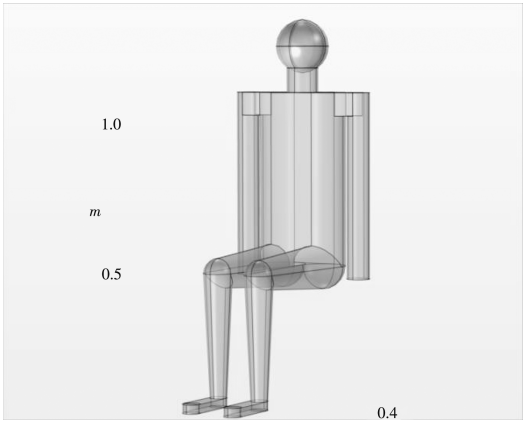

(a) Adult passenger

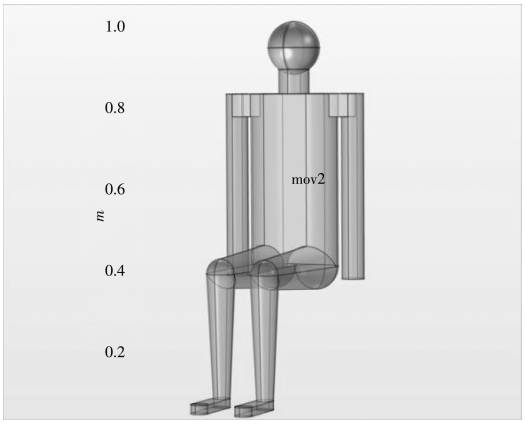

(b) Child passenger

Fig. 5 Human body model

2.3 Model assembly and segmentation

Firstly, all the established models were imported into COMSOL finite element software to assemble, and the child passenger and adult passenger models were placed in the four positions of the electric vehicle co-pilot, left, center and right, respectively. The relative positions of the driver, passengers, coil and car body are shown in Fig. 6.

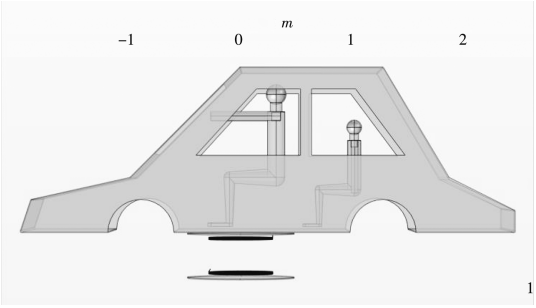

Fig. 6 Position of human coil and car

The simulation calculations were conducted when the passenger was seated at the four positions of the co-driver position, the left position of the rear seat, the central position of the rear seats and the right position of the rear seats.

Secondly, the obtained material properties and dielectric parameters were applied to the air area, the vehicle body, the coils and the human tissues. When the 85 kHz frequency simulation was performed in the AC/DC module and a current of 30 A was applied to the coil, the got input power was about 3.7 kW. The boundary absorption conditions were added. The finite element mesh was divided for different regions and the refined mesh processing was performed on the three-layer ball head model established to make the results more accurate for concentrating the electromagnetic exposure of the human head. The result of the child body dissection is shown in Fig. 7. The meshing of the overall model is shown in Fig. 8.

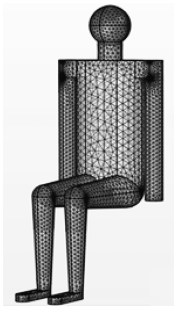

Fig. 7 Result chart of child body dissection

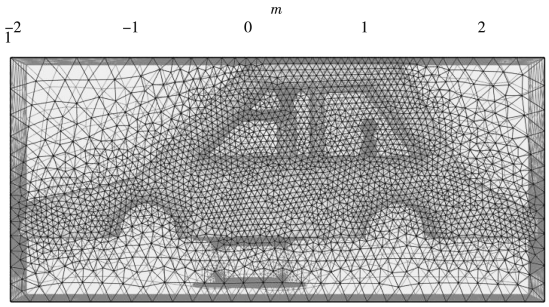

Fig. 8 Overall model splitting result graph

Finally, the wireless charging of EVs was solved in the AC/DC module, and the calculation results were processed. The total degree of freedom to solve the electromagnetic exposure safety assessment model for passengers by wireless charging systems for EVs was about 1.37 million. It took about 30 minutes to complete the solution by a 16 G computer.

3 Results and discussion

3.1 Safety assessment of electromagnetic exposure for child passenger

1) Distribution of magnetic induction intensity in body and head of a child

When the child passenger was in position one (the co-driver position), the magnetic induction intensity and electric field intensity distribution of the human torso are shown in Fig. 9.

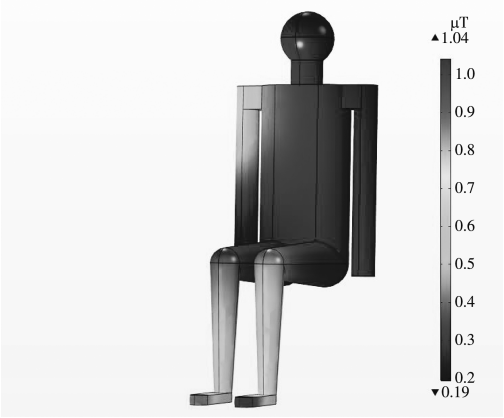

(a) Child body magnetic induction intensity distribution

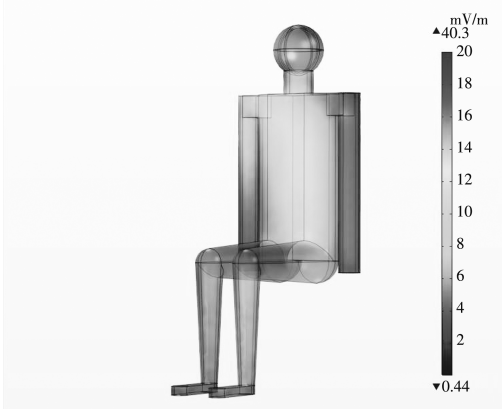

(b) Bhild body induced electric field intensity distribution

Fig. 9 Distribution of child body magnetic induction intensity and induced electric field intensity

The maximum magnetic induction intensity was 1.052 4 μT, which accounted for 16.84% of the ICNIRP threshold. The maximum electric field strength was 0.345 8 mV/m, which accounted for 0.000 4% of the ICNIRP threshold. The maximum value appeared at the toe. The magnetic induction intensity of the right shoulder was larger because the right shoulder was close to the window, the shielding

effect of the window was weaker than that of the car body. The electric field distribution at the left foot and right shoulder was greater than that at other parts. Because at this position, the left half of the human body was closer to the charging coil, and the right shoulder was closed to the window, the values of the two parts were higher. The car body had shielding effect, so the electromagnetic exposure of other parts of human were lower here.

The distribution of magnetic induction intensity on the head of child passenger is shown in Fig. 10. The maximum magnetic induction of the head was 0.357 3 μT, which was 5.72% of the ICNIRP threshold. The cross section was perpendicular to the bottom of the car body, and the cross section of the center of the head was took for slice. The magnetic induction intensity of the head increased with the position near the receiving coil. Since the human body is not a magnetic substance and will not affect the distribution of the spatial magnetic field, the magnetic induction intensity decreases as the distance increases, so the intensity of the magnetic induction intensity of the human head is generally lower than that of the human foot.

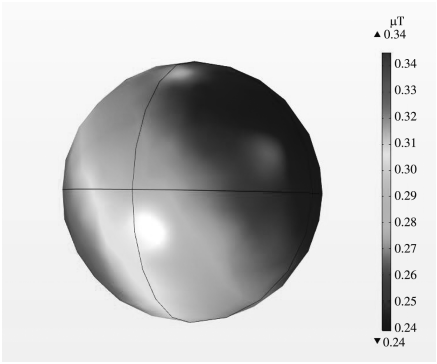

(a) Child head magnetic induction intensity distribution

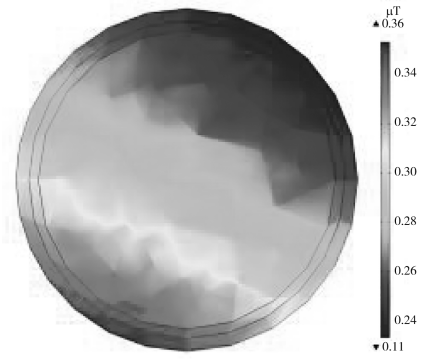

(b) Magnetic induction intensity distribution of longitudinal section of child head

Fig. 10 Child passenger head magnetic induction intensity distribution

The distribution of the induced electric field intensity on the head of a child passenger is shown in Fig. 11. The electromagnetic exposure in front and right sides of the head were greater. The maximum value of the induced electric field intensity was 6.031 8 mV/m, which accounted for 0.006 9% of the ICNIRP threshold. The volume diagram and the slice diagram of the electric field distribution showed that the electromagnetic exposure of the passenger's head was more serious in the front near the windshield of the car and near the right window. Since near the car window electromagnetic shielding effect was small.

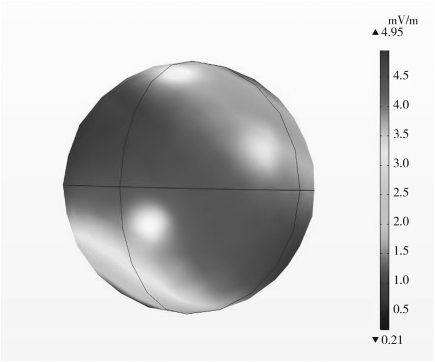

(a) Head induced electric field intensity distribution

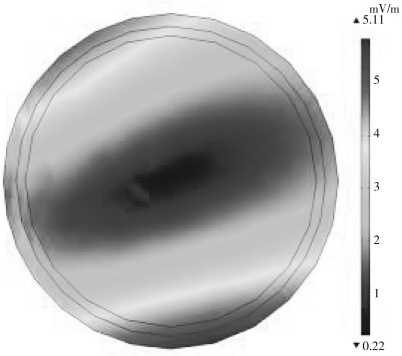

(b) Induction electric field intensity distribution of longitudinal section of head

Fig. 11 Induced electric field intensity distribution on head of child passenger

2) The magnetic induction intensity and induced electric field distribution in the brain tissue of the child passenger

The distribution of magnetic induction intensity of the brain tissue of a child passenger is shown in Fig. 12. Taking a slice perpendicular to the bottom of the car, and the magnetic induction intensity inside the brain tissue increased as it approached the receiving coil.

The distribution of the induced electric field strength of the brain tissue of child passenger is shown in Fig. 13. Taking all sides perpendicular to the bottom of the car and face forward, the maximum value was 5.008 6 mV/m, which accounted for 0.74% of the ICNIRP threshold. The electric field distribution of the brain was similar to that of the

head, with greater exposure on the right and front sides. And because the protective effect of the scalp on the brain, the induced electric field intensity of the brain was slightly lower than that of the entire head.

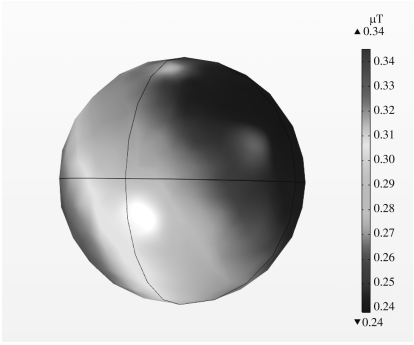

(a) Magnetic induction intensity distribution of brain tissue of child passenger

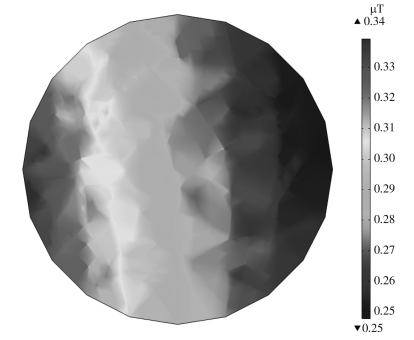

(b) Magnetic induction intensity distribution of brain tissue slices of child passenger

Fig. 12 Magnetic induction intensity distribution of brain tissue of child passenger

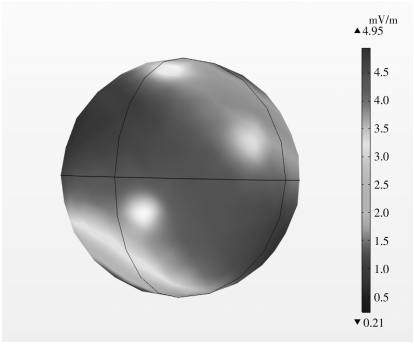

(a) Distribution of induced electric field in brain tissue of child passenger

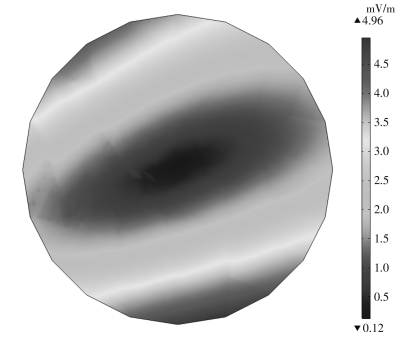

(b) Distribution of induced electric field in brain tissue slices of child passenger

Fig. 13 Induced electric field intensity distribution of child passenger brain tissue

3.2 Comparison of electromagnetic exposure in co-driver position

1) Comparison of human body magnetic induction

As shown in Fig. 14, the maximum values of magnetic induction for adult passengers and child passenger are 1.664 4 μT and 1.052 4 μT, respectively. The magnetic induction in adult passenger is slightly larger. There is no great difference in the magnetic induction intensity of the body between adults and children.

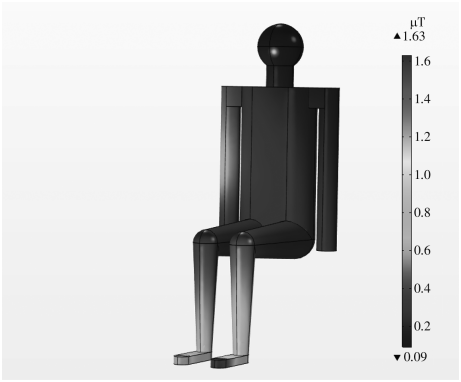

(a) Distribution of magnetic induction intensity for adult passenger

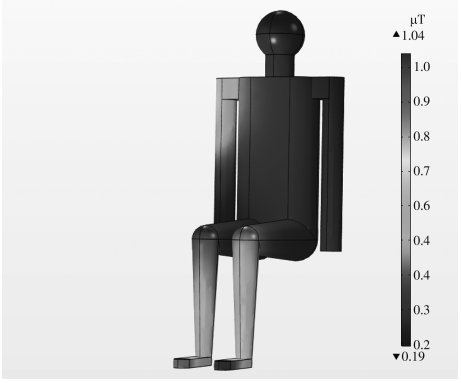

(b) Distribution of magnetic induction intensity for child passenger

Fig. 14 Passenger body magnetic induction intensity distribution

2) Comparison of magnetic induction intensity of brain tissue

A cross-section of the center of the head used for cutting was taken, which was parallel to the bottom of the vehicle body. As shown in Fig. 15, the maximum magnetic induction intensities of adult passenger brain tissue and child passenger brain are 0.168 5 μT and 0.339 3 μT. At the same location, the maximum value of the magnetic induction intensity of the child passenger is about twice as many as that of the adult passenger. Since the shielding effect of the window is smaller than that of the car body, the magnetic induction intensity of the passengers' brain is larger near the window, and slightly smaller at the distance away from the window.

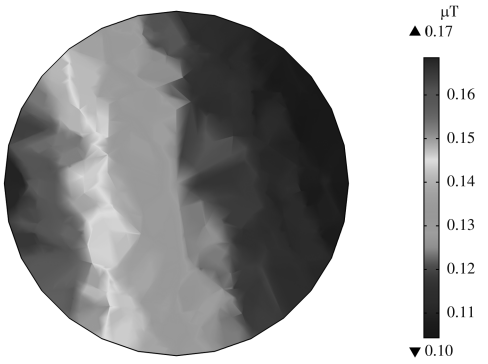

(a) Adult passenger brain tissue magnetic induction intensity distribution

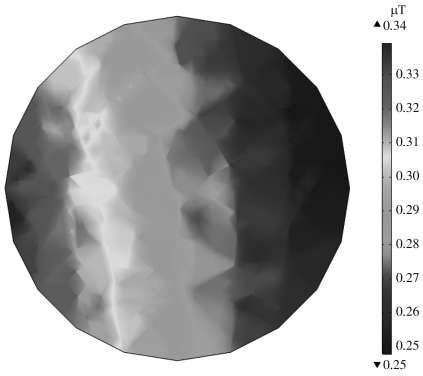

(b) Magnetic induction intensity distribution of brain tissue of child passenger

Fig. 15 Magnetic induction intensity distribution of passenger brain tissue

3) Comparison of body induced electric field strength

As shown in Fig. 16, the maximum value of the induced electric field strength of an adult passenger is 55.972 9 mV/m, and the maximum value of the induced electric field strength of a child passenger is 54.439 1 mV/m. The induced electric field strength of the brain of adult passenger is slightly larger than that of child passenger.

4) Comparison of induced electric field intensity of brain tissue

A cross-section of the center of the head used for cutting was taken, which was parallel to the bottom of the vehicle body. As shown in Fig. 17, the electric field intensity gradually decreased from the outside to the inside, and the maximum values of the electric field strength of the adult passenger brain tissue and the child passenger brain tissue were 3.163 3 mV/m and 4.974 1 mV/m. The maximum electric field intensity in the brain tissue of the child passenger was larger than that of the adult passenger brain tissue. The electrical conductivity of the brain of child passenger was greater than that of adult, resulting in a greater intensity of the induced electric field in the brain of child than that of adult.

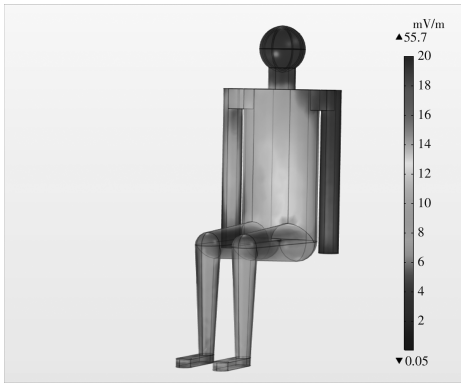

(a) Adult passenger induced electric field strength

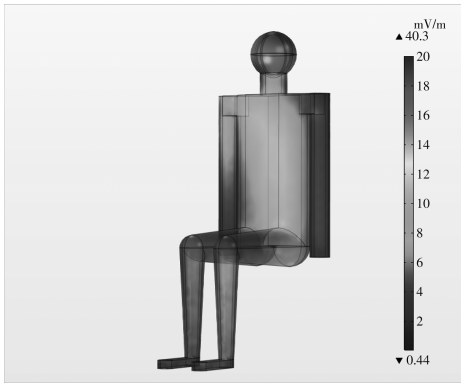

(b) Induced electric field strength of child passenger

Fig. 16 Comparison of human induced electric field

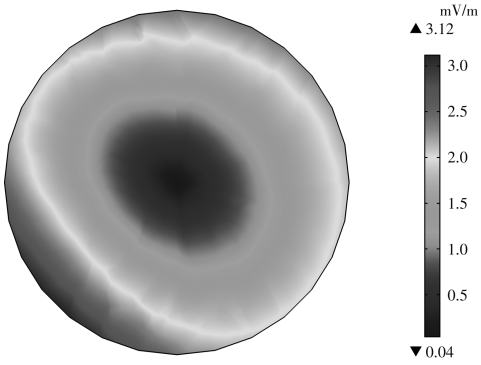

(a) Adult passenger brain tissue electric field intensity distribution

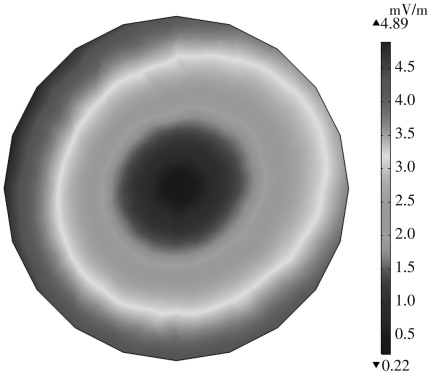

(b) Electric field intensity distribution of brain tissue of child passenger

Fig. 17 Electric field intensity distribution of passenger brain tissue

3.3 Comparison in different positions of rear seats

The adult passenger and the child passenger were placed in the three seats of the rear seats of the electric vehicle in turns. Tables 5—6 list the magnetic induction intensity and induce electric field intensity of the body and brain of the passenger in four different positions. It was found that all the results were below the ICNIRP threshold by calculation. The following is the electromagnetic exposure of the human body and brain of children and adults (magnetic induction intensity and induced electric field intensity).

Table 5 Maximum magnetic induction and maximum electric field strength of human body

Parameter	Type	Position			
		Left rear seat	Central rear seat	Right rear seat	Co-pilot
Magnetic induction /μT	Adult	0.411 0	0.392 6	0.674 7	1.664 4
	Child	0.467 3	0.444 4	0.753 9	1.052 4
Induced electric field strength/(mV·m^{-1})	Adult	67.549 0	50.697 7	76.409 8	55.972 9
	Child	65.072 2	43.815 0	53.627 4	54.4371

Table 6 Maximum magnetic induction intensity and induced electric field intensity of brain tissue sections

Parameter	Type	Position			
		Left rear seat	Central rear seat	Right rear seat	Co-pilot
Magnetic induction /μT	Adult	0.086 1	0.088 3	0.129 9	0.177 4
	Child	0.145 0	0.144 2	0.246 2	0.345 8
Induced electric field strength/(mV·m^{-1})	Adult	1.779 1	1.915 0	2.710 2	3.330 6
	Child	2.045 1	2.004 6	3.584 4	4.974 1

As can be seen from Table 5, the maximum magnetic induction intensity of child passenger's body is slightly larger than that of adult passenger when they sat in the same position. The maximum value of the induced electric field strength is less than that of the adult passenger. Moreover, as the distance between the passenger and the charging coil increases, the magnetic induction intensity and the induced electric field intensity generated in the body decreased. It can be seen from the comparison between the maximum value of the magnetic induction intensity and the maximum value of the induced electric field intensity in the body. Due to the different dielectric parameters and size of the body between the child and the adult, the intensity of the magnetic induction intensity in the body is higher than that of the adult passengers sitting in the same position while the difference of induced electric field intensity is small.

It can be seen from Table 6 that the electromagnetic exposure values of passenger brain tissues are all below the ICNIRP threshold, and the maximum value of the magnetic induction intensity in the brain tissue of the child passenger is about twice than that of the adult passenger sitting in the same position. At the same location, the intensity of the induced electric field in the brain of child passengers is greater than that of adult passengers. Moreover, as the distance between the passenger and the charging coil increases, the magnetic induction intensity and the induced electric field intensity generated in the brain tissue decreased. All calculation results showed that the electromagnetic exposure dose to child passengers is greater than that of adult passengers.

4 Conclusions

This article mainly studied the electromagnetic exposure difference between child passengers and adult passengers during wireless charging of electric vehicles, calculated the child's body dielectric parameters, and simulation calculations were performed in the COMSOL software to compare its exposure level with that of adults.

The child passenger suffered the largest electromagnetic exposure dose in the co-driver position. the distribution of magnetic induction intensity in children's brain tissues is related to the position of the riding position and the position of the wireless charging coil. As the distance of the head from the coil increases, the values of magnetic induction and induced electric field intensity are

decreasing.

The electromagnetic exposure dose of adult passenger is the largest when it is in the co-driver position. The magnetic induction intensity in the body and brain tissue of the child passenger is twice or more than that of the adult passenger at the same position, while the intensity of the induced electric field is not much different from the value of the adult passenger at the same position.

The magnetic induction strength and induced electric field strength of child passenger and adult passenger do not exceed the limits specified of the ICNIRP standard. Due to the incomplete electromagnetic parameters of the children, more extensive research is needed in the future. During the wireless charging process of electric vehicles, it is recommended that children do not ride in the car.

References

[1] KUMAR M S, REVANKAR S T. Development scheme and key technology of an electric vehicle: an overview. Renewable & Sustainable Energy Reviews, 2016, 70(4): 1266-1285.

[2] IMURA T, OKABE H, UCHIDA T, et al. Wireless power transfer during displacement using electromagnetic coupling in resonance. IEEJ Transactions on Industry Applications, 2010, 130(1): 76-83.

[3] LI Y, YANG Q X, CHEN H Y, et al. Basic study on improving power of wireless power transfer via magnetic resonance coupling. Advanced Materials Research, 2012, 459: 445-449.

[4] ZHANG X, YANG Q X, CUI Y, et al. Design, optimization and verification of energy transmitting coils in high-power wireless power transmission systems. Transactions of China Electrotechnical Society, 2013, 28: 12-18.

[5] ANDRÉ K, ARISTEIDIS K, MOFFATT R, et al. Wireless power transfer via strongly coupled magnetic resonances. Science, 2007, 317(5834): 83-86

[6] LAAKSO I, TSUCHIDA S, HIRATA A, et al. Evaluation of SAR in a human body model due to wireless power transmission in the 10 MHz band. Physics in Medicine and Biology, 2012, 57(15): 4991-5002.

[7] LAAKSO I, HIRATA A. Evaluation of the induced electric field and compliance procedure for a wireless power transfer system in an electrical vehicle. Physics in Medicine and Biology, 2013, 58(21): 7583-7593.

[8] LAAKSO I, HIRATA A, FUJIWARA O. Computational dosimetry for wireless charging of an electrical vehicle. Tokyo, 2014: 202-205.

[9] SHIMAMOTO T, LAAKSO I, HIRATA A. Internal electric field in pregnant-woman model for wireless power transfer systems in electric vehicles. Electronics Letters, 2015, 51(25): 2136-2137.

[10] PARK S W. Dosimetry for resonance-based wireless power transfer charging of electric vehicles. Journal of Electromagnetic Engineering & Science, 2015, 15(3): 129-133.

[11] PARK S W. Influence of fields and SAR evaluation for 13.56 MHz EV resonance-based wireless power charging systems. Microwave & Optical Technology Letters, 2017, 59(4): 937-941.

[12] PARK S W. Evaluation of electromagnetic exposure during 85 kHz wireless power transfer for electric vehicles. IEEE Transactions on Magnetics, 2018, 54(1): 1-8.

[13] YAVOLOVSKAYA E, CHIQOVANI G, GABRIADZE G, et al. Simulation of human exposure to electromagnetic fields of inductive wireless power transfer systems in the frequency range from 1 Hz to 30 MHz//International Symposium on Electromagnetic Compatibility, Sep. 5-9, 2016, IEEE, Poland, Europe. Washington: IEEE Computer Society, 2016: 491-496.

[14] YAVOLOVSKAYA E, WILLMANN B, CHIQOVANI G, et al. Low frequency human exposure analysis for automotive applications//International Symposium on Electromagnetic Compatibility, Aug. 4-12, 2016, IEEE, Gaithersburg, USA. Washington: IEEE Computer Society, 2017: 4-8.

[15] XU G Z, LI C X, ZHAO J, et al. Research on electromagnetic environment safety of electric vehicle charging with wireless power transfer. Transactions of China Electrotechnical Society, 2017, 32(22): 152-157.

[16] GAO Y, FARLEY K B, TSE Z T H. Investigating safety issues related to electric vehicle wireless charging technology//Transportation Electrification Conference and Expo (ITEC), Aug. 31-Sep. 3, 2014, IEEE, Beijing, China. Washington: IEEE Computer Society, 2014: 1-4.

[17] HE Y Q, DIAO Y L, SUN W N, et al. Impact of magnetic-field generated by wireless power transfer of electric vehicles on brain waves and neuro-psychological changes//Asia-Pacific International Symposium on Electromagnetic Compatibility (APEMC), May 17-21, 2016, IEEE, Shenzhen, China. Washington: IEEE Computer Society, 2016: 639-641.

[18] ZHANG X, YANG Q X, CHEN H Y, et al. Modeling and design and experimental verification of contactless power transmission systems via electromagnetic resonant coupling. Proceedings of the CSEE, 2012, 32(21): 153-158.

[19] NAOKI S. Wireless power transmission progress for electric vehicle in Japan//Radio and Wireless Symposium (RWS), Jan. 20-23, 2013, IEEE, Austin, TX, USA. Washington: IEEE Computer Society, 2013: 109-111

[20] International Commission on Non-Ionizing Radiation Protection (ICNIRP). International commission on non-ionizing radiation protection guidelines for limiting exposure to time-varying electric, magnetic, and electromagnetic fields (up to 300 GHz). Health Physics, 1998, 74(4): 494-522.

[21] ICNIRP Safety Guideline. Guidelines for limiting expo-

sure to time varying electric and magnetic fields (up to 300 GHz). Health Physics, 2010, 99: 818-836.
[22] GABRIEL C, GABRIEL S, CORTHOUT E. The dielectric properties of biological tissues: I. Literature survey. Physics in Medicine and Biology, 1996, 41(11): 2231-2249.
[23] GABRIEL S, LAU R W, GABRIEL C. The dielectric properties of biological tissues: II. Measurement in the frequency range 10 Hz to 20 GHz. Physics in Medicine and Biology, 1996, 41(11): 2251-2269.
[24] PEYMAN A, REZAZADEH A A, GABRIEL C. Changes in the dielectric properties of rat tissue as a function of age at microwave frequencies. Physics in Medicine and Biology, 2001, 46(6): 1617-1629.
[25] PEYMAN A, HOLDEN S J, WATTS S, et al. Dielectric properties of porcine cerebrospinal tissues at microwave frequencies: in vivo, in vitro and systematic variation with age. Physics in Medicine and Biology, 2007, 52(8): 2229-2245.
[26] RUSH S, DRISCOLL D A, DRISCOLL M E E, et al. Current distribution in the brain from surface electrodes. Anesthesia and Analgesia, 1968, 47(6): 717-723

电动汽车无线电力传输对儿童和成人电磁辐射的比较

康海霞

(兰州交通大学 光电技术与智能控制教育部重点实验室, 甘肃 兰州 730070)

摘 要: 为研究儿童乘客与成人乘客之间的电磁辐射差异, 以验证儿童乘客的安全性, 在 85 kHz 的工作频率下计算出儿童乘客身体的介电参数, 使用有限元模拟软件 COMSOL Multiphysics 建立了电动汽车模型、充电线圈模型、儿童乘客模型和成人乘客模型。当儿童乘客和成人乘客分别坐在汽车的 4 个不同位置时, 分析在身体和头部产生的磁感应强度和感应电场强度的分布, 以及儿童和成人的大脑电磁暴露值之间的差异, 并将其与设定限值进行了比较。实验结果表明: 当乘客在副驾驶位置时, 受到的电磁暴露最大。同一位置儿童的电磁暴露水平略高于成年人, 并且两者的磁感应强度和感应电场强度均远小于设定的公共电磁暴露推荐值。

关键词: 电动汽车; 电磁辐射; 儿童模型; 无线充电线圈; 有限元方法

引用格式: KANG Haixia. Comparison of electromagnetic exposure to child and adult from electric vehicle wireless power transmission. Journal of Measurement Science and Instrumentation, 2022, 13(2): 242-252. DOI: 10.3969/j.issn.1674-8042.2022.02.014